Available online at www.sciencedirect.com
ScienceDirect
Marine Chemistry 106 (2007) 272–286
MARINE CHEMISTRY
www.elsevier.com/locate/marchem

Statistical process control in assessing production and dissolution rates of biogenic silica in marine environments

Marc Elskens [a,*], Anouk de Brauwere [a], Charlotte Beucher [b,1], Rudolph Corvaisier [b], Nicolas Savoye [a,2], Paul Tréguer [b], Willy Baeyens [a]

[a] *Laboratory for Analytical and Environmental Chemistry, Vrije Universiteit Brussel, Pleinlaan 2 B-1050 Brussels, Belgium*
[b] *CNRS UMR 6539, Laboratoire des Sciences de l'Environnement Marin, Université de Bretagne Occidentale, Institut Universitaire Européen de la Mer, Technopôle Brest-Iroise, Place Copernic, 29280 Brest, France*

Received 22 September 2005; received in revised form 30 October 2006
Available online 26 January 2007

Abstract

This paper provides pieces of advice on the practices of quality assurance and quality control in assessing production and dissolution rates of biogenic silica in marine waters with stable isotope techniques. The objective is to make a rigorous contribution to the interpretation of ^{30}Si isotopic measurements including modelling and uncertainty analyses. The results are illustrated with real data taken from Beucher et al. [Beucher, C., Tréguer, P., Corvaisier, R., Hapette, A/-M., Elskens, M., 2004a. Production and dissolution of biogenic silica in a coastal ecosystem of western Europe. Marine Ecology Progress Series 267:57–69.]. Prior to the flux rate assessment, there are a number of analytical considerations required for screening between optimal and defective experimental conditions. Three indexes were proposed to check the relevance of underlying assumptions when dealing with ^{30}Si tracer enrichment and dilution techniques. Afterwards for extracting rate values from measurements, it is necessary to postulate a model, and if required an optimization method. Various models and formulae were compared for their precision and accuracy. It was shown that oversimplified models risk bias when their underlying assumptions are violated, but overly complex models can misinterpret part of the random noise as relevant processes. Therefore, none of the solutions can *a priori* be rejected, but each should statistically be assessed with hypothesis testing. A weighted least squares regression strategy combining an analysis of the standardized residuals and cost function (sum of the weighted least squares residuals) was used to select optimal solution subsets corresponding to a given data set, i.e. the solution that uses the most relevant processes and which was tested for the presence of outliers (observations or measurements with undue influence in the flux rate assessment).

Keywords: Tracer method; Stable isotope; Biogenic silica; Modelling

1. Introduction

Since the pioneering work of Goering et al. (1973), stable isotopes ^{29}Si and ^{30}Si have been used to assess transformation rates of biogenic silica ($BSiO_2$) and silicic acid (H_4SiO_4) in several marine ecosystems (Nelson and Gordon, 1982; Nelson et al., 1991). Later the development of radioactive ^{32}Si isotope measuring

* Corresponding author.
E-mail address: melskens@vub.ac.be (M. Elskens).
[1] Now at: Marine Science Institute, University of California, Santa Barbara, California 93106, United States.
[2] Now at: OASU, UMR EPOC, Université Bordeaux 1, CNRS, Station Marine d'Arcachon, 33120 Arcachon, France.

0304-4203/$ - see front matter © 2007 Elsevier B.V. All rights reserved.
doi:10.1016/j.marchem.2007.01.008

procedures (Tréguer et al., 1991; Brzezinski and Phillips, 1997) has significantly improved the measurements of biogenic silica production rates (e.g. Brzezinski et al., 1998; Quéguiner, 2001). However, there are several reasons to further use stable isotopes in routine measurements; (1) their use remains the only way to measure silica dissolution rates, and (2) they are not hazardous. This does not exclude that some inherent difficulties remain, for example, measuring rates of near surface silica dissolution with isotope dilution and mass spectrometry remains a difficult task because this rate may be low, especially in offshore waters. It is anticipated that increased experimental ingenuity will overcome some of these technical difficulties. In that way, refined analytical methods were recently developed based on thermal ionisation-mass spectrometry, TI-MS (Corvaisier et al., 2005) and high resolution-inductively coupled plasma-mass spectrometry, HR-ICP-MS (Klemens and Heumann, 2001; Cardinal pers. comm.).

In order to extract values for the flux rates (production and dissolution of biogenic silica) from those measurements, it is necessary to postulate a model. In addition, an appropriate optimization method should be chosen with care since the numerical values for the parameter estimates largely depend upon the criteria and methods used to match model and measurements (Janssen and Heuberger, 1995). Because pathways that control nutrient cycling in aquatic systems are seldom univocal, there is understandably some disagreement about the best approach to model these processes (number of parameters, number of equations…). The first goal of this paper is to compare the estimation behaviour of the basic model approach for assessing silicic acid uptake by phytoplankton (Nelson and Goering, 1977a) and silica dissolution (Nelson and Goering, 1977b) with a nonlinear two compartmental model previously described in Beucher et al. (2004a,b) and de Brauwere et al. (2005a). Since the notion of a "true model" is typically a fiction for real-life application, usefulness rather than trueness should be the guiding principle in developing and comparing models. Clearly, there is a need for criteria allowing an objective assessment of the model results (Elskens et al., 2005) and a well-defined model selection strategy (de Brauwere et al., 2005b). Therefore, the second goal of this paper is to present a series of data processing techniques that are relevant from a user's and management's perspective. Namely, which strategy should be applied to select an appropriate model solution? How can systematic errors or model failure be detected with real data? What confidence can be placed into the final model outcome? Which data can be considered as outliers and should be removed?

The result of this quality assessment is illustrated with real data reported in Beucher et al. (2004a) and discussed in relation to quality assurance for research and development and non-routine analysis.

2. Material and methods

2.1. Experimental design and assumptions

The enrichment and isotope dilution technique, which is applied for the simultaneous determination of biosilica production and dissolution rates, involves the addition of enriched $Na_2^{30}SiO_3$ solutions to a water sample, and after some period of incubation measuring (i) the ^{30}Si incorporated into the particulate material (=uptake) and (ii) the coincident tracer dilution in the dissolved pool due to dissolution of unlabelled biosilica. The changes in concentration and isotopic abundance of H_4SiO_4 acid and $BSiO_2$ are assessed by measuring them just after the spike ($t=0$) and after a given incubation period, usually 24 h. Isotopic abundance is defined as 100% $[^{30}Si]/([^{28}Si]+[^{29}Si]+[^{30}Si])$. The analytical procedures are described in Corvaisier et al. (2005). Before these measurements can be interpreted, a number of basic statements about the behaviour of the isotopic tracer must be postulated: (i) the tracer undergoes the same transformations (transfer reactions) as the unlabelled substrate, i.e. isotope effects are negligible, (ii) there is no exchange of the isotope between the labelled substance and other substances in the system, (iii) the tracer is initially not in equilibrium with the system under study, and its change over time is quantifiable, (iv) regeneration has the background ratio of abundance, i.e. it consists of non-enriched compounds, and (v) the tracer addition does not perturb the steady state existing in the system as a whole, i.e., there are no significant perturbations to compartments and their transformations.

These are basic assumptions in experimental designs involving isotope enrichment and dilution procedures (e.g. Harrison, 1983). For silicon isotopes, assumptions (i–ii) are not seriously violated (De La Rocha et al., 1997). Although assumptions (i) and (iv) may appear contradictory, it is not. The rationale of assumption (iv) is the following. In order to solve the model equations, the abundance at which dissolution of $BSiO_2$ proceeds must be fixed. By the uptake of H_4SiO_4, diatoms build up their frustules composed of amorphous silica. While diatoms are alive, an organic coating protects silica from dissolution (Bidle and Azam, 1999). It is usually

assumed that only dead diatoms can dissolve. Moreover, Beucher et al. (2004b) showed that the dissolution rate correlated to the percentage of dead diatom. It is, therefore, reasonable that a finite period of time is required before any of the ^{30}Si-enriched atoms will appear in the regenerated H_4SiO_4. The validity of assumption (iii) may be a problem when long incubation period is used and abundance of the tracer, as well as concentration of the labelled substrate change substantially. Violation of assumption (iv) also becomes significant under these circumstances. For assumption (v), "true" tracer additions, considered usually as <10% of the ambient concentration (Dugdale and Goering, 1967), is not always achievable. As a consequence, changes in substrate concentration and flux rates may be significant. To what extend violations of those assumptions will create significant biases in flux rate calculations will undoubtedly vary between systems, but several criteria are useful for screening between optimal and defective experimental conditions (see Section 2.3).

2.2. Model description

For the sake of clarity all symbols used hereafter are defined in the glossary and their notations applied throughout.

2.2.1. The Nelson and Goering formulae

The classical approach for assessing silicic acid uptake by phytoplankton (Nelson and Goering, 1977a) and silica dissolution (Nelson and Goering, 1977b) is derived from the following one compartmental model:

$$\overset{(\phi,æ_\phi)}{\rightarrow}[C\ æ_C] \tag{1}$$

The differential equations associated with this model are:

$$\begin{cases} \dfrac{\partial æ_C}{\partial t} = -\dfrac{(æ_C(t)-æ_\phi)\cdot\phi}{C(t)} \\ \dfrac{\partial C}{\partial t} = \phi \end{cases} \tag{2}$$

Straightforward integration of Eq. (2) yields the following mass and isotopic balances:

$$\begin{cases} æ_C(t)\cdot C(t) = æ_C(0)\cdot C(0) + æ_\phi\cdot\phi\cdot t \\ C(t) = C(0) + \phi\cdot t \end{cases} \tag{3}$$

Eq. (3) can be rewritten with appropriate symbols for an enrichment experiment in the particulate phase according to:

$$\begin{aligned} &C = BSiO_2;\quad æ_C(0) = 0;\quad æ_C(t) = æ_{BSiO_2}(t);\\ &æ_\phi = æ_{H_4SiO_4}(0);\quad \phi = u \end{aligned} \tag{4}$$

or for an isotope dilution experiment in the dissolved phase according to:

$$\begin{aligned} &C = H_4SiO_4;\quad æ_C(0) = æ_{H_4SiO_4}(0);\\ &æ_C(t) = æ_{H_4SiO_4}(t);\quad æ_\phi = 0;\quad \phi = d \end{aligned} \tag{5}$$

From Eqs. (3)–(5), uptake of H_4SiO_4 and dissolution rates of $BSiO_2$ can be solved for as follows:

$$u = \begin{cases} \dfrac{BSiO_2(t)\cdot æ_{BSiO_2}(t)}{t\cdot æ_{H_4SiO_4}(0)} \\ \dfrac{BSiO_2(0)\cdot æ_{BSiO_2}(t)}{t\cdot(æ_{H_4SiO_4}(0)-æ_{BSiO_2}(t))} \end{cases}$$

$$d = \begin{cases} \dfrac{H_4SiO_4(t)\cdot(æ_{H_4SiO_4}(0)-æ_{H_4SiO_4}(t))}{t\cdot æ_{H_4SiO_4}(0)} \\ \dfrac{H_4SiO_4(0)\cdot(æ_{H_4SiO_4}(0)-æ_{H_4SiO_4}(t))}{t\cdot æ_{H_4SiO_4}(t)} \end{cases} \tag{6}$$

Similar formulae have widely been applied to compute nitrogen (Dugdale and Goering, 1967; Dugdale and Wilkerson, 1986; Collos, 1987) and carbon (Collos and Slawyk, 1985; Legendre and Gosselin, 1996) transport rates in aquatic systems. It is noted, however, that two different analytical solutions were gathered whether considering the sample concentration at the beginning or the end of the incubation. Conceptually, these solutions should be mathematically equivalent if the model correctly described the main features of production and dissolution processes. In many cases, however, it is an approximation, and differences between formulae (6) may be ascribed to concentration changes over the incubation period and isotope dilution effects. To correct for concentration changes, Nelson and Goering (1977a,b) recommend the use of the geometric mean in computing rates:

$$\begin{cases} u = \dfrac{(BSiO_2(O)\cdot BSiO_2(t))^{0.5}\cdot æ_{BSiO_2}(t)}{t\cdot æ_{H_4SiO_4}(0)} \\ d = \dfrac{(H_4SiO_4(0)\cdot H_4SiO_4(t))^{0.5}\cdot(æ_{H_4SiO_4}(0)-æ_{H_4SiO_4}(t))}{t\cdot æ_{H_4SiO_4}(0)} \end{cases} \tag{7}$$

Alternatively, it is possible to handle both isotope dilution and concentration changes with compartmental analysis (Beucher et al., 2004a,b; de Brauwere et al., 2005a).

2.2.2. Two compartmental model for $BSiO_2$ production and dissolution

$$[H_4SiO_4\ æ_{H_4SiO_4}] \underset{(d,æ_{BSiO_2})}{\overset{(u,æ_{H_4SiO_4})}{\rightleftharpoons}} [BSiO_2\ æ_{BSiO_2}] \tag{8}$$

Important features of model (8) are that all Si atoms that leave the dissolved phase are assumed to appear as

particulate silica, and that dissolution is regarded as a process that transfers Si atoms from the particulate to the dissolved pool. Analogous models or even more complicated ones were build-up to address the problem of N cycling in aquatic systems (Elskens et al., 2005). The differential equations associated with the two compartment model are:

$$\begin{cases} \dfrac{\partial H_4SiO_4}{\partial t} = d-u \\ \dfrac{\partial æ_{H_4SiO_4}}{\partial t} = -d \cdot \dfrac{æ_{H_4SiO_4}(t)}{H_4SiO_4(t)} \\ \dfrac{\partial BSiO_2}{\partial t} = u-d \\ \dfrac{\partial æ_{BSiO_2}}{\partial t} = d \cdot \dfrac{æ_{BSiO_2}(t)}{BSiO_2(t)} + u \cdot \dfrac{æ_{H_4SiO_4}(t)-æ_{BSiO_2}(t)}{BSiO_2(t)} \end{cases} \quad (9)$$

When Eq. (9) is integrated, the relevant model equations are:

$$\begin{cases} H_4SiO_4(t) = H_4SiO_4(0) + (d-u)\cdot t \\ æ_{H_4SiO_4}(t) = æ_{H_4SiO_4}(0) \cdot \left(1 + \dfrac{d-u}{H_4SiO_4(0)} \cdot t\right)^{\dfrac{d}{u-d}} \\ BSiO_2(t) = BSiO_2(0) + (u-d)\cdot t \\ æ_{BSiO_2}(t) = \dfrac{æ_{H_4SiO_4}(0)\cdot H_4SiO_4(0)}{BSiO_2(0) + (u-d)\cdot t} \cdot \left(1-\left(1 + \dfrac{d-u}{H_4SiO_4(0)} \cdot t\right)^{\dfrac{u}{u-d}}\right) \end{cases} \quad (10)$$

There are several methods to extract rates from this system, since it involves four equations for merely two unknowns (u and d). Due to random and systematic variations, there are differences between model results and measurements. Therefore, the best method is to seek those parameter-values that minimize all four equations simultaneously, instead of solving 1 or 2 equations analytically. However, due to the second and the fourth equations in Eq. (10), the model is nonlinear in the unknowns. To be solved an iterative optimization algorithm must then be used.

It is noted that with the current experimental design only the averaged rate over the incubation period can be determined, i.e. $\phi(u,d) = \frac{1}{t}\int_0^t \phi(t)\cdot \mathrm{d}t$. This is true independently of the chosen model structure. To assess instantaneous rates $\phi(t)$, a mechanism (e.g. first, second order, or saturation kinetic) for the transformation reactions must be postulated, but this requires time-series measurements.

2.3. Rules for the screening of experimental conditions

In Section 2.1, we have summarized 5 characteristics of the behaviour of an "ideal" tracer to perform isotope enrichment and dilution experiments. Violations of these assumptions may generate significant biases in the rate calculations. If isotope equilibrium is reached or approached during an experiment, one cannot warrant the flux rate-values (violation of assumption iii). For the system under study, isotope equilibrium is achieved after ^{30}Si enrichment, when the abundance of the particulate phase ($BSiO_2$) and dissolved phase (H_4SiO_4) becomes equal; the tracer is then said to be in a steady state. A useful measure of this is given by the abundance ratio AR, a rescaled index varying between 0 and 1:

$$AR = \frac{æ_{H_4SiO_4}(t)-æ_{BSiO_2}(t)}{æ_{H_4SiO_4}(0)} \quad (11)$$

When AR is close to 1, the tracer is far from equilibrium (optimal conditions). When AR moves towards zero, the tracer approaches steady state conditions. There are only informal guidelines for thresholds under which values of AR should require attention. We suggest to highlight the data when AR < 0.25. Likewise, a simple index (HL) based on the half-life and incubation period (Δt) can be used to gauge the validity limit of assumption (iv).

$$HL = \frac{BSiO_2(0)}{2\cdot d\cdot \Delta t} \quad (12)$$

with $BSiO_2$ the biogenic Si concentration and d the dissolution rate.

If HL becomes ≤ 1 (i.e. more than half of the $BSiO_2$ pool is recycled during the incubation time), violation of assumption (iv) becomes likely, and the data should be highlighted. Violations of (iii and iv) are often interrelated, and it is not unusual for a dataset to be highlighted by both criteria. Under these conditions, the likelihood of gross errors is so serious that there is no real alternative than to reject the result of the experiment. Finally when the tracer addition (TA) is > than 10% of the ambient H_4SiO_4 concentration (violation of assumption v), flux rates should be considered as potential ones.

2.4. Assessment of model accuracy

In order to assess the discrepancy between the observations y_i and the model counterparts $f_{\mathrm{model}}(x_i,\theta)$, we need some way to transform the residual $(y_i - f_{\mathrm{model}}(x_i,\theta))$ to a common scale on which we know what large and small values are. An obvious approach is to define a standardized residual:

$$SR_i = \frac{y_i - f_{\mathrm{model}}(x_i,\theta)}{\sigma_i} \quad (13)$$

where σ_i should express the total standard deviation of the residual. This is achieved here by linearization of the

input noise on x_i and adding them to the original output noise on y_i (de Brauwere et al., 2005a):

$$\sigma_i^2 = \sigma_{y,i}^2 + \sum_{i=1}^{n} \left| \frac{\partial f_{\text{model}}(x_i, \theta)}{\partial x_i} \right|^2 \cdot \sigma_{x,i}^2 \quad (14)$$

Substituting the u- and d-estimates from models (1) and (8) in their corresponding mass balance Eqs. (3) and (10) yields standardized residuals for concentration and abundance in the dissolved and particulate phases. We choose the standardized residuals for two reasons. Firstly, SR_i solves the problem of scaling, i.e. if y_i and σ_i^2 are good estimates of the population's mean and variance, then the SR_i's can be interpreted as standard normal deviates. The accuracy of the models towards measurements was further assessed by inspecting the SR_i distribution for a series of 53 experiments carried out by Beucher et al. (2004a). If the models correctly describe the main features of uptake and dissolution processes, it is expected that RS_i-scores will be symmetrically distributed with a mean of zero. Moreover, the meaning of the scores can be immediately appreciated, e.g., absolute values of $RS_i \leq 1$ would be very common ($\approx$68% of the data) whereas absolute values of $RS_i > 3$ would be very rare (<0.27% of the data) suggesting either model failure or outlying measurements. This enables a direct comparison between models that are solved algebraically and numerically. Secondly SR_i has a natural interpretation in the context of the residual cost function CF, which is used to estimate the model parameters in model (8):

$$\text{CF} = \sum_{i=1}^{n} \text{SR}_i^2 \approx \sum_{i=1}^{n} (N(0,1))^2 = \chi_{n-p}^2 \quad (15)$$

Depending on the assumption of the normal distribution, which outliers apart seems to be justified in practice, the CF has a chi-squared χ^2 distribution with $n-p$ degrees of freedom (Box, 1970; Rod and Hancil, 1980), where n stands for the number of measurements and p for the number of parameters in the model. With this information, it is possible to assess the "probability" of a residual cost function value. If the residual value falls beyond a chosen confidence limit, the results should be rejected for being "unlikely" (de Brauwere et al., 2005b). For instance, if the residual value is significantly higher than expected, the remaining difference between model and measurements is too high to be explained only by stochastic measurement noise. This significant difference between the expected and observed residual cost function is an indicator of systematic errors, and is thus complementary to the SR_i approach. Moreover, as will be discussed later, the cost function approach is also useful for selecting relevant parameters within a given model.

2.5. Assessment of model precision

Knowledge of model precision is necessary for the effective judgment of the model results (e.g. comparison with specification limits) and for inter-comparison of different model outcomes. From the outset, all the factors that may contribute to uncertainty in the model calculations are expressed as standard deviations. While it cannot always be taken for granted that there exits a regular functional relationship between precision and the concentration level of an analyte, the Horwitz function has shown that the relative standard deviation (RSD) is useful in evaluating precision over a wide range of concentration (Horwitz, 1983; Thompson and Lowthian, 1997). For H_4SiO_4 determinations, Strickland and Parsons (1968) reported RSD values close to 2.5%. For $BSiO_2$ determinations, Ragueneau and Tréguer (1994) reported RSD values close to 10%. For isotopic analysis, results obtained on Na_2SiO_3 standard solution indicated RSD less than 0.5% (Corvaisier et al., 2005). However, actual precision may be lower than the quoted value, particularly with ^{30}Si enriched sample that has been processed through all steps of the incubation protocol. An overall RSD of 2% appears, therefore, reasonable in estimating the Si isotopic composition of both $BSiO_2$ and H_4SiO_4. Model precision (propagation of random error in calculations) is assessed with Monte-Carlo simulations. A number of random deviates (500) on concentrations and isotopic ratios were generated by computer assuming normal distributions with known mean and RSD. For each random deviation, the Si flux rates were calculated resulting in a distribution of best fit parameter values from which the statistical properties can be analyzed, and thus a quantification of the model precision can be achieved.

3. Results and discussion

3.1. Screening of experimental conditions

An examination of the data according to the rules defined in Section 2.3 does not indicate any outliers out of the 53 experiments. The median for the AR, HL and TA indexes amount to 0.9, 7 and 13, respectively which are not far from optimal values ($AR \approx 1$; $HL \gg 1$; $TA \leq 10\%$; Fig. 1). However of these experiments, two

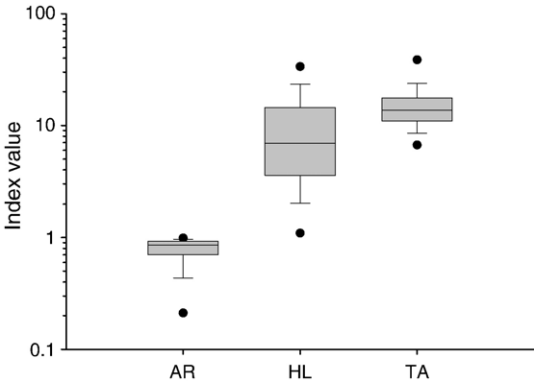

Fig. 1. Index values for the series of 53 experiments carried out by Beucher et al. (2004a). Optimal conditions are characterised by AR ≈ 1 (tracer is not in equilibrium), HL ≫ 1 ($T_{1/2}$ of $BSIO_2$ is much greater than the incubation period) and TA ≤ 10% (tracer addition is less than 10% of the ambient H_4SIO_4). The boxes, whiskers and symbols cover the twenty-fifth to seventy-fifth, the tenth to ninetieth and the fifth to ninety-fifth percentiles, respectively.

were characterized by an AR index < 0.25, meaning that the tracer approaches steady state conditions (violation of assumption iii), two by a HL index < 1, meaning that more than half of the $BSIO_2$ pool was recycled over the incubation period (violation of assumption iv), and 42 by tracer additions >than 10% of the ambient H_4SiO_4 (violation of assumption v). There are 12 missing data for the ^{30}Si abundance of H_4SiO_4 at the end of the experiment. Hence, the comparison of model results for dissolution will be carried out on the 41 remaining data.

3.2. Model comparison

The main aim of model comparison is the identification of systematic variations or bias, i.e. does one model or formula give results that are significantly higher or lower than the other one? We first consider the analytical solutions issued from the Nelson and Goering's model (Eq. (6)), either based on concentrations determined at the beginning (u_{NGI}, d_{NGI}) or at the end of the experiment (u_{NGF}, d_{NGF}). From Fig. 2, it appears that (u_{NGI}, d_{NGI}) are systematically greater than their corresponding (u_{NGF}, d_{NGF}). For both rates, the absolute differences between the solutions are log-normally distributed, and statistically significant in more than 25% (box plot, upper quartile range, Fig. 2). Implicit in Eq. (6) are the conditions leading to these major discrepancies (period between May and September 2001):

$$\left\{\begin{array}{l} u>0 \\ d\rightarrow u \end{array}\right. \Rightarrow \left\{\begin{array}{l} \left.\begin{array}{l} BSiO_2(t)\approx BSiO_2(0) \\ æ_{H_4SiO_4}(0) > æ_{H_4SiO_4}(0) - æ_{BSiO_2}(t) \end{array}\right\} \Rightarrow u_{NGI} \gg u_{NGF} \\ \left.\begin{array}{l} H_4SiO_4(t)\approx H_4SiO_4(0) \\ æ_{H_4SiO_4}(0) > æ_{H_4SiO_4}(t) \end{array}\right\} \Rightarrow d_{NGI} \gg d_{NGF} \end{array}\right.$$

Nelson and Goering (1977a,b) themselves pointed out that results may differ depending on whether the initial or final concentration is used in calculations. Instead, they recommended using the geometric mean of the concentration over the course of incubation (Eq. (7)). Fig. 3 compares results from these upgraded formulae (u_{NGGM}, d_{NGGM}) with those derived from the two compartmental model (u_{2CM}, d_{2CM}). Clearly u_{NGGM} yields an underestimated rate since it does not allow for possible H_4SiO_4 production during incubation. Put in another way, any conditions that lead to a significant $BSiO_2$ dissolution during the experiment tend to dilute the ^{30}Si at.% enrichment of the H_4SiO_4 pool, and therefore to significantly underestimate the uptake rate (period between May and September 2001, Fig. 3). Only models such as Eq. (8), which take into account the time dependence of the isotopic ratio in each compartment, enable correcting for isotope dilution. The importance of this process for reliable N uptake assessment was recognised as well (see Elskens et al., 2005 and references therein). Yet when the dissolution rate decreases (period between October 2001 and February 2002), much better agreements between u_{NGGM} and u_{2CM} are found. In contrast herewith, no systematic variations between d_{NGGM} and d_{2CM} were observed (Fig. 3). The difference between both rates fluctuates randomly throughout the sampling period following a normal distribution. Summarising the aforementioned results, it can be stated that:

$$\left.\begin{array}{l} d>0 \Rightarrow æ_{H_4SiO_4}(0) > æ_{H_4SiO_4}(t) \Rightarrow u_{NGGM} \ll u_{2CM} \\ d\rightarrow 0 \Rightarrow æ_{H_4SiO_4}(0) \approx æ_{H_4SiO_4}(t) \Rightarrow u_{NGGM} \rightarrow u_{2CM} \end{array}\right\} d_{NGGM} = d_{2CM} \pm \varepsilon$$

where ε is the random residual term.

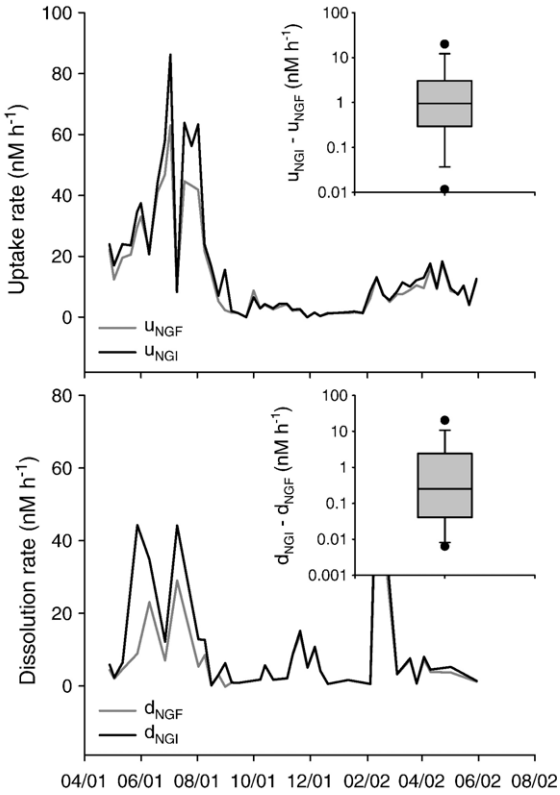

Fig. 2. Comparison between rates issued from the Nelson and Goering's formulae either based on concentrations determined at the beginning or at the end of the experiment (Eq. (6)). The boxes, whiskers and symbols cover the twenty-fifth to seventy-fifth, the tenth to ninetieth and the fifth to ninety-fifth percentiles, respectively.

Model comparisons allow identification of bias and conditions that increase error margins, but do not yield quantitative information on the reliability of the solutions. It is important to have some indication of the quality of the model results, and in particular to demonstrate their fitness for the purpose in hand. This is expected to include the degree to which a result would be expected to agree with other results, normally irrespective of the parameterization used. Useful measures of this are the model precision and accuracy.

3.3. Model precision

Model precision concerns the propagation of experimental uncertainties throughout rate calculations, and is function of the model parameterizations. Fig. 4 shows the standard uncertainty (SU) on the flux rates for the whole set of experiments. While there is no evidence for a systematic difference between models for SU on the uptake rate (Wilcoxon Signed Rank test, $p=0.06$), there is a statistically significant difference (Wilcoxon Signed Rank test, $p \leq 0.001$) for SU on the dissolution rate with $SU_{NGGM>}$ SU_{2CM}. This is due to the fact that the two compartment model (8) uses the whole available information (four equations for two unknowns), and therefore is better constrained than model (1), especially when the ^{30}Si abundance of H_4SiO_4 at the beginning and end of incubation do not significantly differ. Monte-Carlo simulations were performed here to conduct an objective assessment of the model precision; each models being treated in a same way (Section 2.5). In both cases, however, valid approximations of the model uncertainty can be obtained using simpler forms. For model (1), classical rules for combining standard uncertainty in linear and multiplicative expressions are summarized in Ellison et al. (2000). For model (8), refined uncertainty estimation using the parameter covariance matrix was given by de Brauwere et al. (2005a).

3.4. Model accuracy

Model accuracy is the closeness of agreement between the model predictions and the observations, and incorporates both random and systematic variations. It provides a measure of the confidence that can be

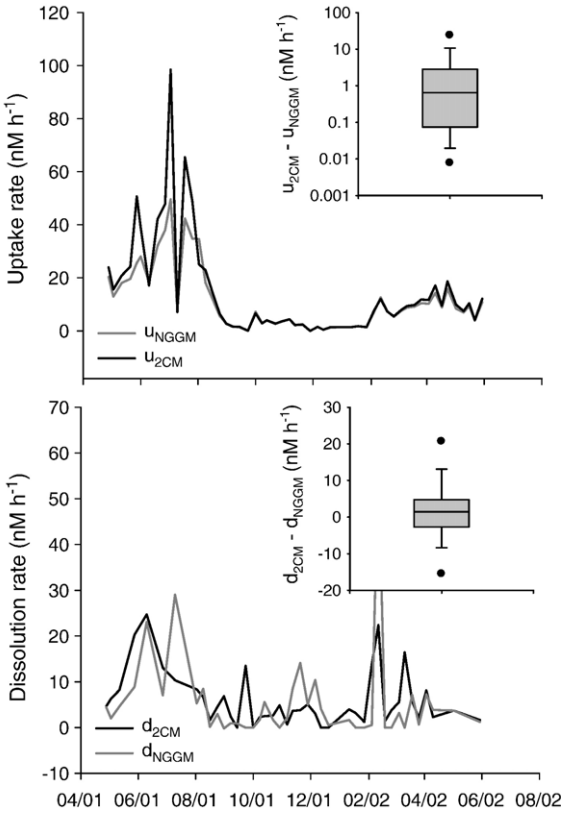

Fig. 3. Comparison between rates issued from the upgrading formulae of Nelson and Goering (Eq. (7)) and the two compartmental model (Eq. (8)). The boxes, whiskers and symbols cover the twenty-fifth to seventy-fifth, the tenth to ninetieth and the fifth to ninety-fifth percentiles, respectively.

placed on a model result. In order to test the model accuracy, we first utilized the standardized residual technique (Eq. (13)). For the upgraded Nelson and Goering's formulae (Eq. (7); Fig. 5a), the RS_i-scores do not behave as standard normal variables. Rather, the distributions are skewed, medians mainly differ from 0, and there are too many unacceptable scores. As discussed in the next section, a high score value can reflect an outlying measurement. Thought, when more than 25% of the score distribution is >3, there are

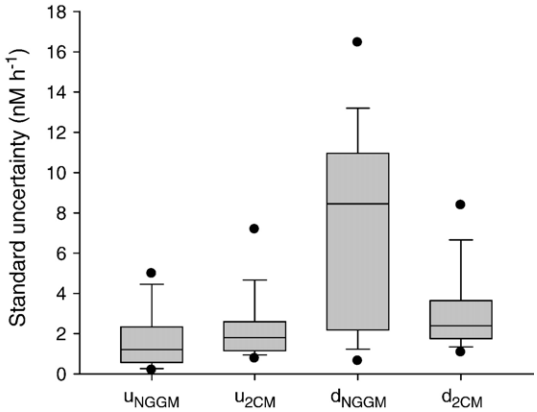

Fig. 4. Standard uncertainty (SU) on flux rates calculations for model (1) and model (8). SU-values were computed with Monte-Carlo simulations as described in the text. Subscripts *u* and *d* stand for uptake and dissolution rates. The boxes, whiskers and symbols cover the twenty-fifth to seventy-fifth, the tenth to ninetieth and the fifth to ninety-fifth percentiles, respectively.

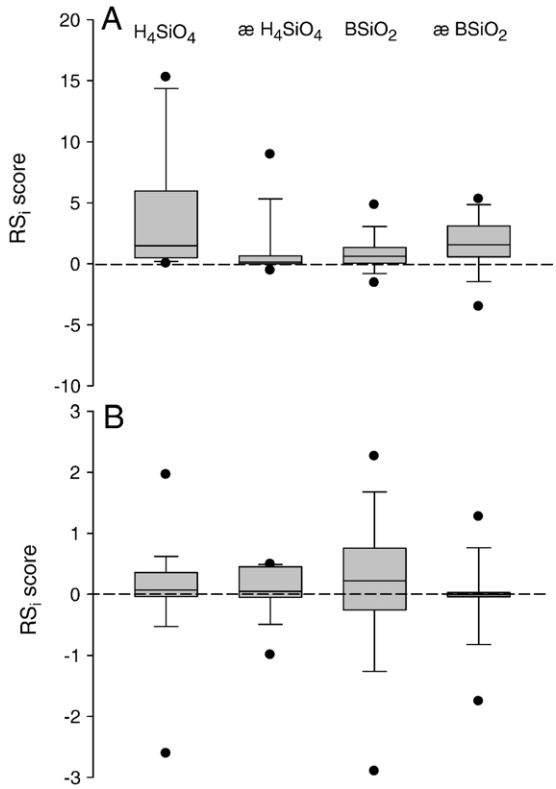

Fig. 5. RS_i-scores for models (1) and (8). (A) Upgraded Nelson and Goering's formulae, (B) Outcomes of the two compartment model. Absolute value of RSi > 3 indicates unacceptably poor model performance in terms of accuracy while for a satisfactory performance $|RSi| \leq 2$ is required. The boxes, whiskers and symbols cover the twenty-fifth to seventy-fifth, the tenth to ninetieth and the fifth to ninety-fifth percentiles, respectively.

evidence for model failures as observed between May and September 2001. Under these conditions, the difference between the model fits and measurements is too high to be explained by random variations only. On the other hand, the RS_i-scores for the two compartment model better fit to the ideal zero-centred distribution (Fig. 5b): there is no evidence of systematic errors.

Some additional values were attached to methods of combining scores. For example the sum of the squared standardized residuals (Eq. (15)) yield an interpretable cost function CF, which behaves as a sample from a χ^2 distribution. To check the overall statistical behaviour, our CF-values for model (8) were compared with the 95–99% percentiles of the χ^2 distribution. In addition, the CF-values were plotted in a histogram, which can easily be compared with the probability density function (pdf) of the χ^2 distribution (Fig. 6). Two observations can be made:

(i) Two measurement sets produce a residual CF greater than the 95th percentile, one of them being even greater than the 99th percentile. According to the Analytical Methods Committee (1992), this means that one result should be rejected ($CF > \chi^2_{99\%}$) and the other one is questionable ($\chi^2_{95\%} < CF \leq \chi^2_{99\%}$). From a statistical point of view, instead of the expected 5 and 1% that exceed the 95 and 99th percentiles, respectively, 4 and 2% do so. This is well acceptable since the 41 measurements do not represent 41 realizations of the same experiment, but correspond to a one year time series. Therefore, the variability is not only due to random noise, but also to environmental changes.

(ii) Apart from these 2 experiments, it is also obvious in both pictures that most of the CF-values are very close to zero. These extreme low values cause a discrepancy between the histogram and the pdf of the χ^2 function. This is probably due to an overestimation of the experimental uncertainties. These latter were indeed used in the cost function to weight the data, which results in a CF-value that is too small in case of overestimated

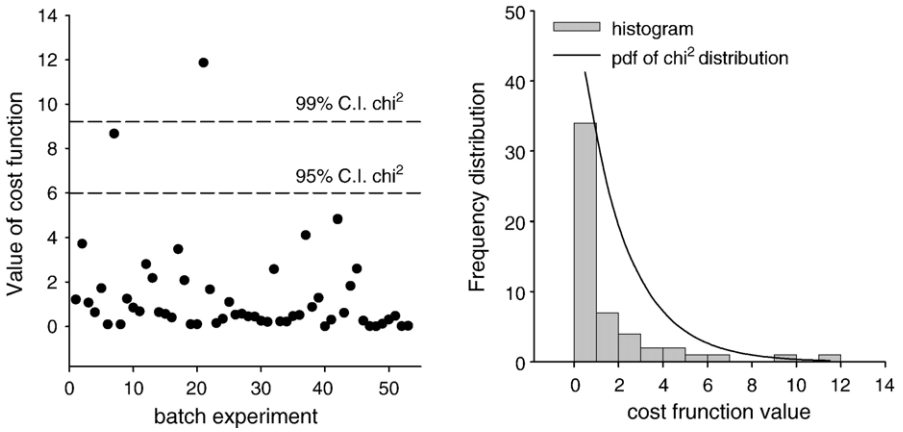

Fig. 6. Cost function values for the series of 53 experiments carried out by Beucher et al. (2004a). The histogram enables a comparison with the χ^2 probability distribution function (pdf).

residual variance (Eq. (14)). Fig. 5b suggests that these overestimations could affect the standard deviations on H_4SiO_4 concentration and on ^{30}Si at.%. For these measurements, the spread of the RS_i distributions is too small. In well behaved systems, the box (50% of the data) and the dots (95% of the data) should approximately extend to ± 1 and ± 2, as reported for the RS_i distribution of $BSiO_2$.

These observations have two main consequences. First, because the CF-value is probably underestimated, the chance of making a Type II error (accepting a wrong model result) increases. Secondly, by propagating overvalued standard deviation through Monte-Carlo simulations, the standard uncertainty on the final model result is overestimated. These points illustrate well the importance for correct estimations of measurement repeatability as outlined by ISO guidelines.

3.5. Handling of outliers

Outliers are extreme observations that for one reason or another do not belong to the other observations in the dataset. If the model equations are routinely applied to these data, then the obtained estimates can be seriously misleading. Hereafter, we present a formal treatment for detecting outliers with undue influence in parameter assessment and demonstrate the serious consequences of failing to detect outliers. The procedure combining the analysis of standardized residuals and cost function is as follows:

1. Optimize parameter-values with the two compartmental model, and compare the residual CF-value to the 99%-quantile of the χ^2 distribution. If the model fit is such that $CF > \chi^2_{99\%}$ go to 2.
2. Analyse the SR_i-scores. If one absolute value of the scores is close to 3 - (the others being ≤ 1), remove it (it is an unusual observation with respect to the others) and repeat step 1 with one degree of freedom less (n-p-1). If not go to 3.
3. If several absolute values of the scores are greater than 2, remove one by one (each time keeping the other outlying scores) repeating step 1 with one degree of freedom less $(n-p-1)$. Keep only that model with the lowest CF-value. If not go to 4.
4. When discrimination between various residual CF-values is impossible (e.g. all the values are acceptable and close together), or when the residual cost function remains greater than $>\chi^2_{99\%}$ after data treatment, one cannot warrant the flux rate-values, and the results must be discarded.

In order to illustrate steps 2 to 4, we randomly generated outlying observations in the dataset no. 38 of Beucher et al., 2004a. Under these conditions, the reference rates are known, and can be used to validate the procedure. There are three issues for the interpretation of this outlier simulation test (Table 1). First, in most simulations, the CF-values (initial) lead to the rejection of the model results ($>\chi^2_{99\%}$) and the data were subsequently processed according to steps 2 to 4. In the remaining part, the model results were questionable ($\chi^2_{95\%} < CF \leq \chi^2_{99\%}$), which is not unusual enough to justify further data treatments (e.g. Table 1, #11 and 12). Second, the standardized residuals analysis has revealed in most cases an unusual score with respect to the values of the others. This score was simply removed and the data processed according to step 2. In the

Table 1
Results of the outlier simulation test in the dataset no. 38 of Beucher et al. (2004a)

Input and output variables	Original value	Simulation of outlier	New value	CF initial $df=n-p$	Unusual SR_i scores	CF final $df=n-p-1$	Model solution
				$\leq\chi^2_{95\%}$			accepted
H_4SiO_4 (0)	10.5	#1	9.2	$>\chi^2_{99\%}$	H_4SiO_4	$\leq\chi^2_{95\%}$	accepted
		#2	12.5	$>\chi^2_{99\%}$	H_4SiO_4	$\leq\chi^2_{95\%}$	accepted
æ H_4SiO_4 (0)	6.3	#3	7.8	$>\chi^2_{99\%}$	æ H_4SiO_4	$\leq\chi^2_{95\%}$	Accepted
		#4	5.5	$>\chi^2_{99\%}$	æ H_4SiO_4	$\leq\chi^2_{95\%}$	Accepted
$BSiO_2$ (0)	3.4	#5	2.4	$>\chi^2_{99\%}$	$BSiO_2$	$\leq\chi^2_{95\%}$	Accepted
		#6	5.4	$>\chi^2_{99\%}$	$BSiO_2$	$\leq\chi^2_{95\%}$	Accepted
H_4SiO_4 (t)	10.4	#7	11.7	$>\chi^2_{99\%}$	H_4SiO_4	$\leq\chi^2_{95\%}$	Accepted
		#8	9.1	$>\chi^2_{99\%}$	H_4SiO_4	$\leq\chi^2_{95\%}$	Accepted
æ H_4SiO_4 (t)	6.1	#9	5.3	$>\chi^2_{crit,99\%}$	æ H_4SiO_4	$\leq\chi^2_{95\%}$	Accepted
		#10	7.6	$>\chi^2_{99\%}$	æ H_4SiO_4	$\leq\chi^2_{95\%}$	Accepted
$BSiO_2$ (t)	3.8	#11	2.6	$\leq\chi^2_{99\%}$	–	–	Questionable
		#12	4.9	$\leq\chi^2_{99\%}$	–	–	Questionable
æ $BSiO_2$ (t)	0.6	#13	0.4	$\leq\chi^2_{95\%}$	–	–	Accepted
		#14	4.4	$>\chi^2_{99\%}$	æ H_4SiO_4	$\leq\chi^2_{95\%}$	Rejected
					æ $BSiO_2$	$\leq\chi^2_{95\%}$	

Outliers were randomly generated for each of the input and output variables. Given the degrees of freedom of the system, the procedure described in the text is useful to detect any outlying observation, but one at a time. Symbols CF = cost function; df = degrees of freedom; SR_i = standardized residuals.

remaining data, several scores may appear unusual. Following step 3, the model results corresponding to the lowest value of the cost function are selected or discarded when the CF-values do not differ significantly (e.g. Table 1, #14). Third, the method appears efficient to prevent undue influence in parameter assessment. Fig. 7 shows that almost all rate values (u_{2CM}, d_{2CM}), obtained after outlier removal, fall within the 95% confidence interval of the original data. There is thus no evidence of systematic errors. In contrast herewith, whenever the Nelson and Goering formulae are routinely applied the obtained estimates can be seriously misleading. Given the number of degrees of freedom of the system, the method outlined above is useful to detect any outlying observation, but one at a time. It is not designed for testing several outliers together. It is noted that while the likelihood of having one outlier (absolute value of $RS_i \geq 3$) out of a series of 7 independent measurements is 2.1%, it decreases to 0.63% or 0.19% for 2 or 3 concomitant outliers.

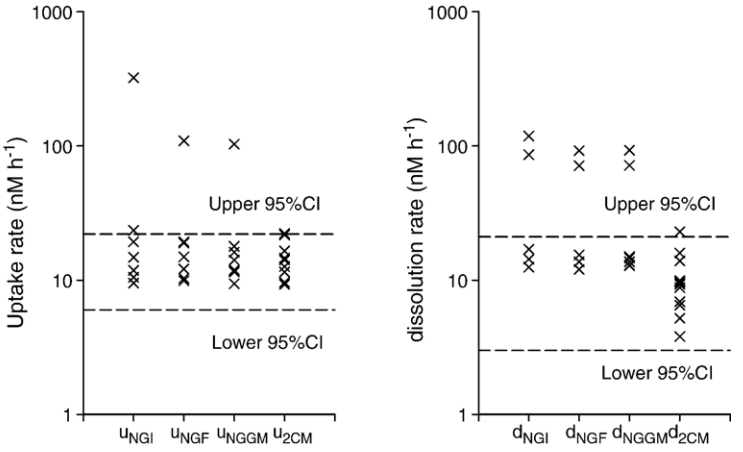

Fig. 7. Flux rates-values for the outlier simulation test. Subscript 2CM stands for the outcomes of the two compartment models involving the outlier detection procedure as described in the text. Subscripts NGI, NGF and NGGM refer to the outcomes of the routinely applied formulae of the Nelson and Goering's model.

Table 2
Results of model selection (MS)

Batch experiment	Date	*d* nM/h	*u* nM/h	*d* nM/h	*u* nM/h	CF	Index			
		Before MS		After MS			AR	HL	TA	
1	28/04/01	6.0±1.4	22.2±1.1	6.0±1.4	22.2±1.1	sat	GS	GS	45	
2	03/05/01	4.4±1.6	15.3±0.9	<MDL	15.7±1.1	que	GS	GS	32	
3	12/05/01	5.6±1.2	20.8±1.2	5.6±1.2	20.8±1.2	sat	GS	GS	16	
4	21/05/01	3.9±3.0	23.4±1.2	<MDL	22.5±1.6	sat	GS	GS	22	md
5	28/05/01	20.2±1.9	50.6±2.6	20.2±1.9	50.6±2.6	sat	0.17	GS	19	
6	01/06/01	11±3.4	38.9±4.0	<MDL	33.2±2.0	sat	GS	GS	53	md
7	10/06/01	23.3±2.6	19±7	26.9±2.3	<MDL	que	GS	GS	36	
8	19/06/01	6.6±3.5	42.1±3.1	<MDL	37.5±2.4	sat	GS	GS	17	md
9	27/06/01	10.5±1.7	46.3±2.2	10.5±1.7	46.3±2.2	sat	GS	GS	18	
10	03/07/01	34.7±6.9	84.6±7.6	34.7±6.9	84.6±7.6	sat	GS	1.0	21	md
11	10/07/01	27.0±3.6	38.9±4.5	27.0±3.6	38.9±4.5	sat	GS	0.8	15	
12	18/07/01	25.8±4.8	54.8±4.7	25.8±4.8	54.8±4.7	sat	GS	GS	13	md
13	26/07/01	13.9±2.1	45.2±3.2	13.9±2.1	45.2±3.2	sat	GS	GS	17	md
14	02/08/01	6.9±1.0	23.7±2.7	6.9±1.0	23.7±2.7	sat	0.19	GS	25	
15	09/08/01	5.6±1.4	20.3±1.4	5.6±1.4	20.3±1.4	sat	GS	GS	16	
16	16/08/01	1.6±1.5	14.9±1.8	<MDL	15.3±1.9	sat	GS	GS	11	
17	24/08/01	1.6±1.9	6.3±1.1	<MDL	7.0±0.8	sat	GS	GS	13	
18	31/08/01	1.4±1.8	2.8±1.2	<MDL	3.6±0.5	sat	GS	GS	GS	
19	07/09/01	1.7±1.3	0.7±1.1	<MDL	2.0±0.2	sat	GS	GS	GS	
20	14/09/01	−0.1±1.6	1.5±0.9	<MDL	1.4±0.2	sat	GS	GS	GS	
21	23/09/01	−4.9±2.2	2.1±1.4	−4.9±2.2	2.1±1.4	uns	GS	GS	11	
22	01/10/01	22.0±2.3	5.7±1.1	<MDL	6.4±0.8	sat	GS	GS	13	
23	08/10/01	2.5±2.1	1.9±1.1	<MDL	2.7±0.7	sat	GS	GS	12	
24	13/10/01	2.2±2.4	2.4±2.2	<MDL	4.2±0.9	sat	GS	GS	GS	
25	22/10/01	−0.2±2.0	3.0±1.0	<MDL	3.0±0.4	sat	GS	GS	13	
26	29/10/01	1.5±1.1	1.2±2.2	1.9±1.0	<MDL	sat	GS	GS	GS	
27	06/11/01	−0.9±3.0	4.9±1.8	<MDL	4.4±0.5	sat	GS	GS	11	
28	12/11/01	3.9±2.4	0.8±1.4	4.4±2.5	<MDL	sat	GS	GS	13	
29	20/11/01	2.2±2.8	1.8±1.4	<MDL	2.7±0.3	sat	GS	GS	13	
30	28/11/01	3.7±8.2	1.2±8.9	2.7±3.1	<MDL	sat	GS	GS	11	
31	06/12/01	2.4±3.6	0.6±1.6	3.4±2.6	<MDL	sat	GS	GS	11	md
32	12/12/01	−0.5±3.7	0.7±1.7	<MDL	0.4±0.2	sat	GS	GS	GS	
33	20/12/01	−2.0±2.2	2.1±1.1	<MDL	1.3±0.2	sat	GS	GS	12	
34	11/01/02	2.6±3.4	0.7±1.4	3.5±2.9	<MDL	sat	GS	GS	16	
35	18/01/02	0.9±3.5	1.4±2.0	<MDL	1.9±0.5	sat	GS	GS	GS	
36	27/01/02	−0.2±4.8	1.5±2.1	<MDL	1.4±1.2	sat	GS	GS	11	
37	04/02/02	3.4±5.9	6.6±3.5	<MDL	8.3±2.2	sat	GS	GS	GS	
38	11/02/02	9.6±6.3	14.1±4.6	<MDL	14.3±2.7	sat	GS	GS	GS	
39	18/02/02	0.5±10.1	7.6±5.8	<MDL	7.3±1.8	sat	GS	GS	GS	
40	25/02/02	1.2±7.0	5.2±2.6	<MDL	5.6±1.3	sat	GS	GS	14	
41	05/03/02	3.0±5.9	7.4±2.3	<MDL	8.4±0.8	sat	GS	GS	18	
42	11/03/02	7.4±8.8	8.4±3.8	<MDL	11.3±1.0	sat	GS	GS	18	
43	19/03/02	3.2±4.6	9.0±1.8	<MDL	10.0±1.2	sat	GS	GS	16	
44	26/03/02	−1.0±4.5	12.5±2.0	<MDL	12.2±1.0	sat	GS	GS	21	
45	03/04/02	4.7±2.7	11.0±1.5	<MDL	12.6±1.1	sat	GS	GS	18	
46	10/04/02	1.4±2.0	16.7±2.0	<MDL	17.3±2.1	sat	GS	GS	11	
47	17/04/02	0.9±2.4	9.2±1.0	<MDL	9.5±0.9	sat	GS	GS	16	md
48	23/04/02	2.3±2.7	18.1±1.2	<MDL	17.7±1.5	sat	GS	GS	18	md
49	02/05/0	3.3±0.9	8.6±0.8	3.3±0.9	8.6±0.8	sat	GS	GS	16	
50	10/05/02	0.8±2.2	7.2±0.7	<MDL	7.4±0.7	sat	GS	GS	17	md
51	16/05/02	4.6±2.2	8.9±1.2	<MDL	9.7±1.0	sat	GS	GS	14	md
52	22/05/02	1.2±1.4	3.7±0.7	<MDL	4.0±0.5		GS	GS	17	md
53	30/05/02	0.9±1.4	11.4±1.9	<MDL	11.4±2.0		GS	GS	GS	

Datasets from Beucher et al. (2004a). Symbols: CF = cost function, sat = satisfactory ($CF \leq \chi^2_{95\%}$), que = questionable ($\chi^2_{95\%} < CF \leq \chi^2_{99\%}$), uns = unsatisfactory ($CF > \chi^2_{99\%}$), MDL = model detection limit, AR = abundance ratio, HL = half-life of $BSiO_2$, TA = tracer addition relative to the H_4SiO_4 ambient level (%), md = missing data, GS = good status for the index under consideration ($AR \approx 1$; $HL \gg 1$; $TA \leq 10\%$).

3.6. Reliability of the model solutions

When judged by the overall performance (precision, accuracy and robustness), model (1) clearly failed when compared to Eq. (8). It should be noted, however, that the analytical solutions of Eq. (1) correspond to peculiar solutions of Eq. (8) when u or d are equal to 0. Because such conditions may occur, we do not reject Eq. (1) in general but need a model selection strategy to decide when a parameter can be cancelled without losing the information hidden in the measurements. Put in another way, oversimplified models such as Eq. (1) risk bias when their underlying assumptions are violated, but overly complex models such as Eq. (8) can misinterpret part of the random noise as relevant processes.

To select optimal solutions subsets corresponding to a given data set, we applied a procedure recently proposed by de Brauwere et al. (2005b), combining a statistical interpretation of the cost function and the principle of parsimony. The approach provides a sound basis for model selection because it is well recognized that other things being equal, the greater the number of parameters, the greater the extent of nonlinear behaviour, the worse the model predictability (Ratkowsky, 1990). The optimized parameter values obtained after model selection are shown in Table 2. Several remarks can be made:

(i) After selection, uptake and dissolution rates were respectively removed from the model equations in respectively 11 and 66% of the experiments. It is important to appreciate that this does not mean that the rates equal zero, only that they cannot be reliably quantified. Hence they should be regarded as censored data (below the model detection limit).

(ii) The standard uncertainty on the remaining parameters is mostly lower than before selection (Wilcoxon Signed Rank test, $p \leq 0.001$). This is one of the rewards using model selection: by reducing the number of parameters, the uncertainty on the remaining parameters decreases.

(iii) Rate values are given for the 12 datasets for which the ^{30}Si abundance of H_4SiO_4 or/and $BSiO_2$ was missing. This is allowed because with one missing data, there is still one degree of freedom left ($n-p-1$) and the model is constrained.

Furthermore, Table 2 summarizes information on the various index types used to estimate the measurements, such as the abundance ratio (AR), the half-life of $BSiO_2$ (HL) and the tracer addition (TA). Combined with the CF approach, this information indicates which reliability can be given to the final results.

4. Conclusions and final remarks

This paper provides advice on the concepts and practices of quality assurance and quality control when validating a model result. Whilst these guidelines were illustrated with model results based on the ^{30}Si tracer methodology, they have wider applications, e.g. tracer enrichment and dilution experiments.

It was emphasized that isotope enrichment and dilution models belong to a class of compartmental models for which the governing law is mass conservation. They are described by a set of differential equations, and their structure is categorized as stochastic since any variables in the model can be expressed by a probability distribution. Therefore, estimating the model parameters with a weighted least squares technique allows improving the accuracy of the parameter values, making them less sensitive to outlying observations. Standardized residuals that have normal distributions, and sum of the weighted least square residuals that have χ^2 distributions are matching techniques (easily interpretable with significance tests) for determining whether a model result is satisfactory or not. Additionally, there are a number of analytical and experimental considerations on experimental design (abundance ratio, half-life, tracer addition indexes) and measurement uncertainty (repeatability of analytical methods), which are needed for a correct model assessment. Combining these approaches with significance testing allows us to judge the quality of the model results.

5. Glossary

Symbols	Definition	Units
æ's	^{30}Si at.% enrichment in the various Si compartments or associated with the corresponding flux rates as indicated by the subscript	%
C	Concentration of the Si compartments	μM
$BSiO_2$	Concentration of biogenic silica	μM
H_4SiO_4	Concentration of silicic acid	μM
ϕ	Si flux rates	μM h^{-1}
u	Uptake rate of H_4SiO_4	μM h^{-1}
d	Dissolution rate of $BSiO_2$	μM h^{-1}
$(0, t)$	Initial and final times of the incubation period	h
AR	Abundance ratio index	–
HL	Half-life index of $BSiO_2$	–
TA	Tracer addition index	%
CF	Cost function (=sum of the squared residuals)	–
$f_{model}(x_i,\phi)$	The ith model forecast	μM or %

n	The number of model equations	–
p	The number of parameters to be estimated in a given model	–
SR_i	The standardized residual	–
SU	The standard uncertainty	μM/h
x_i	The ith input variable	μM or %
y_i	The ith output variable	μM or %
σ_i	Standard deviation of the ith residual	–
$\sigma_{x,j}$	Standard deviation of the jth input variable	μM or %
$\sigma_{y,j}$	Standard deviation of the jth ouput variable	μM or %
$\partial y_i/\partial x_j$	The partial differential of y_i with respect to x_j	–

Acknowledgments

This paper is dedicated to the memory of Roland Wollast, who guided the first steps of Marc Elskens in IGBP and Global Change related Research in Belgium (1989–95). This research was conducted under grant GOA22/DSCHWER4 as part of the project Geconcerteerde Onderzoekacties supported by the Vrije Universiteit Brussel.

References

Analytical Methods Committee, 1992. Proficiency testing of analytical laboratories: organization and statistical assessment. Analyst 117, 97–117.

Beucher, C., Tréguer, P., Corvaisier, R., Hapette, A.-M., Elskens, M., 2004a. Production and dissolution of biogenic silica in a coastal ecosystem of western Europe. Marine Ecology Progress Series 267, 57–69.

Beucher, C., Tréguer, P., Corvaisier, R., Hapette, A.-M., Pichon, J.-J., Metzl, N., 2004b. Intense summer biosilica recycling in the Southern Ocean. Geophysical Research Letters 31. doi:10.1029/2003GL.018998.

Bidle, K.D., Azam, F., 1999. Accelerated dissolution of diatom silica by marine bacterial assemblages. Nature 397, 508–512.

Box, M.J., 1970. Improved parameter estimation. Technometrics 12, 219–229.

Brzezinski, M.A., Phillips, D.R., 1997. Evaluation of Si-32 as a tracer for measuring silica production rates in marine waters. Limnology and Oceanography 42, 856–865.

Brzezinski, M.A., Villareal, T.A., Lipschultz, F., 1998. Silica production and the contribution of diatoms to new and primary production in the central North Pacific. Marine Ecology Progress Series 167, 89–104.

Collos, Y., 1987. Calculations of ^{15}N uptake rates by phytoplankton assimilating one or several nitrogen sources. Applied Radiation and Isotopes 38, 275–282.

Collos, Y., Slawyk, G., 1985. On The compatibility of carbon uptake rates calculated from stable and radioactive isotope data — implications for the design of experimental protocols in aquatic primary productivity. Journal of Plankton Research 7, 595–603.

Corvaisier, R., Tréguer, P., Beucher, C., Elskens, M., 2005. Determination of the rate of production and dissolution of biosilica in marine waters by thermal ionisation mass spectrometry. Analytica Chemica Acta 534, 149–155.

de Brauwere, A., De Ridder, F., Elskens, M., Schoukens, J., Pintelon, R., Baeyens, W., 2005a. Refined parameter and uncertainty estimation when both variables are subject to error. Case study: estimation of Si consumption and regeneration rates in a marine environment. Journal of Marine Systems 55, 205–221.

de Brauwere, A., De Ridder, F., Pintelon, R., Elskens, M., Schoukens, J., Baeyens, W., 2005b. Model selection through a statistical analysis of the minimum of a Weighted Least Squares cost function. Chemometrics and Intelligent Laboratory Systems 76, 163–173.

De La Rocha, C.L., Brzezinski, M.A., De Niro, M.J., 1997. Fractionation of silicon isotopes by marine diatoms during biogenic silica formation. Geochimica et Cosmochimica Acta 61 (23), 5051–5056.

Dugdale, R.C., Goering, J.J., 1967. Uptake of new and regenerated forms of nitrogen in primary productivity. Limnology and Oceanography 12, 196–206.

Dugdale, R.C., Wilkerson, F.P., 1986. The use of ^{15}N to measure nitrogen uptake in eutrophic oceans; experimental considerations. Limnology and Oceanography 31, 673–689.

Ellison, S.L.R., Rosslein, M., William, A. (Eds.), 2000. Quantifying Uncertainty in Analytical Measurement, EURACHEM/CITAC Guide CG4. UK Dep. of Trade and Ind., London. 120 pp.

Elskens, M., Baeyens, W., Brion, N., De Galan, S., Goeyens, L., de Brauwere, A., 2005. Reliability of n flux rates estimated from ^{15}N enrichment and dilution experiments in aquatic systems, Global Biogeochemical Cycles 19, GB4028.

Goering, J.J., Nelson, D.M., Carter, J.A., 1973. Silicic acid uptake by natural populations of marine phytoplankton. Deep-Sea Research 20, 777–789.

Harrison, W., 1983. Nitrogen in the marine environment: Use of isotopes. In: Carpenter, E.J., Capone, D.G. (Eds.), Nitrogen in the Marine Environment. Academic Press, Inc., pp. 763–808.

Horwitz, W., 1983. Today's chemical realities. Journal of AOAC International 66, 1295–1301.

Janssen, P.H.M., Heuberger, P.S.C., 1995. Calibration of process-oriented models. Ecological Modelling 83, 55–66.

Klemens, P., Heumann, K.G., 2001. Development of an ICP-HRIDMS method for accurate determination of traces of silicon in biological and clinical samples. Fresenius' Journal of Analytical Chemistry 371, 758–763.

Legendre, L., Gosselin, M., 1996. Estimation of N or C uptake rates by phytoplankton using ^{15}N or ^{13}C: revisiting the usual computation formulae. Journal of Plankton Research 19, 263–271.

Nelson, D.M., Goering, J.J., 1977a. A stable Isotope Tracer Method to Measure Silicic Acid Uptake by Marine Phytoplankton. Analytical Biochemistry 78, 139–147.

Nelson, D.M., Goering, J.J., 1977b. Near-surface silica dissolution in the upwelling region off northwest Africa. Deep-Sea Research 24, 65–73.

Nelson, D.M., Gordon, L.I., 1982. Production and pelagic dissolution of biogenic silica in the Southern Ocean. Geochimica et Cosmochimica Acta 46, 491–500.

Nelson, D.M., Ahern, J.A., Herlihy, L.J., 1991. Cycling of biogenic silica within the upper water column of the Ross Sea. Marine Chemistry 45, 461–476.

Quéguiner, B., 2001. Biogenic silica production in the Australian sector of the Sub-Antartic Zone of the southern Ocean in late summer 1998. Journal of Geophysical Research 106, 31627–31636.

Ragueneau, O., Tréguer, P., 1994. Determination of biogenic silica in coastal waters — applicability and limits of the alkaline digestion method. Marine Chemistry 45, 43–51.

Ratkowsky, D.A., 1990. Handbook of nonlinear regression models. In: Owen, D.B. (Ed.), Statistics: textbooks and Monographs. Marcel Dekker, INC, New York. ISBN: 0-8247-8189-9, p. 241.

Rod, V., Hancil, V., 1980. Iterative estimation of model parameters when measurements of all variables are subject to error. Computers & Chemical Engineering 4, 33–38.

Strickland, J.D.H., Parsons, T.R., 1968. A practical handbook of sweater analysis. In: Stevenson, J.C. (Ed.), Fisheries Research Board of Canada. Bulletin, vol. 167, p. 311.

Thompson, M., Lowthian, P.J., 1997. The Horwitz function revisited. Journal of AOAC International 80, 676–679.

Tréguer, P., Lindner, L., Vanbennekom, A.J., Leynaert, A., Panouse, M., Jacques, G., 1991. Production of biogenic silica in the Weddell–Scotia Seas measured with Si-32. Limnology and Oceanography 36, 1217–1227.